Supplementary Material: The Value of Citizen Science for Flood Risk Reduction: Cost-benefit Analysis of a Citizen Observatory in the Brenta-Bacchiglione Catchment

Michele Ferri[1], Uta Wehn[2], Linda See[3], Martina Monego[1] and Steffen Fritz[3]

[1]Alto-Adriatico Water Authority (AAWA), Cannaregio 4314, 30121 Venice, Italy
[2]IHE Delft Institute for Water Education, Westvest 7, 2611 AX Delft, The Netherlands
[3]International Institute for Applied Systems Analysis (IIASA), Schlossplatz 1, 2361 Laxenburg, Austria

Correspondence to: Michele Ferri (michele.ferri@distrettoalpiorientali.it)

Hydrological and Hydraulic Modelling

The flood forecasting system developed for the Brenta-Bacchiglione River basin ingests meteorological forecasts and couples this with a hydrological-hydraulic model to predict flood events (i.e., water levels in the river, depth of flooding in flooded areas). The hydrological model can run in a continuous mode, fed by meteorological data based on different weather forecasting models (i.e., COSMO, ECMWF, MOLOCH, HIRLAM) or using real-time data. It is also coupled with a snow melt module (UEB - Utah Energy Balance Model (Tarboton and Luce, 1996)) and a data assimilation module to assimilate measured data, including observations sent by the citizen observers (i.e., water levels of the river) (Mazzoleni et al., 2017, 2018).

The hydraulic model uses the HEC-RAS software (a numerical model developed by the US Army Corps of Engineers Hydrologic Engineering Center) and can perform one and two-dimensional hydraulic calculations for a full network of natural and constructed channels. The hydrological model provides the initial boundary conditions to the hydraulic model. The hydraulic model uses geometry acquired from LIDAR data.

The outputs of the model consist of a time series of water levels evaluated at all river cross-sections across all river branches. For each of these river cross-sections, a set of three thresholds has been defined by the Civil Protection authorities. The third threshold refers to the situation when the river will overtop the bank and thus lead to flooding. The system has been used to run rainfall-runoff and hydrodynamic simulations and to provide short-term predictions (2-3 days in advance) to the authorities.

The hydrological model used in this study is part of the early warning system implemented and used by Alto-Adriatico Water Authority (AAWA). A description of the model is provided here but the reader is referred to Ferri et al. (2012) and Mazzoleni et al. (2017) for more detailed descriptions. The hydrological response of the catchment is estimated using a hydrological model that contains routines for runoff generation and a routing procedure. The processes related to runoff generation (i.e., surface, sub-surface, and deep flow) are modelled mathematically by applying the water balance to a control volume representative of the active soil at the sub-catchment scale. The water content, S, in the soil is updated at each calculation step, dt, using the following balance equation:

$$S(t+dt) = S(t) + P(t) - R(t) - R_{sub}(t) - L(t) - E_T(t) \quad (1)$$

where P and E_T are the components of precipitation and evapotranspiration, respectively, while R, R_{sub}, and L are the surface runoff, subsurface runoff, and deep percolation model states, respectively. The surface runoff, R, is based on specifying the critical threshold beyond which the mechanism of Dunnian flow (i.e., the saturation excess mechanism) prevails:

$$R(t) = \begin{cases} C\left(\frac{S(t)}{S_{\max}}\right)P(t) \Rightarrow P(t) \le f = \frac{S_{\max}(S_{\max} - S(t))}{(S_{\max} - CS(t))} \\ P(t) - (S_{\max} - S(t)) \Rightarrow P(t) > f \end{cases} \quad (2)$$

where C is a coefficient of soil saturation obtained by calibration, and S_{max} is the content of water at saturation point, which depends on the nature and use of the soil.

The subsurface flow is considered proportional to the difference between the water content, S, at time, t, and that at soil capacity, Sc:

$$R_{sub}(t) = c(S(t) - S_c) \quad (3)$$

while the estimated deep flow is evaluated according to the expression proposed by Laio et al. (2001):

$$L(t) = \frac{K_s}{e^{\beta\left(1-\frac{S_c}{S_{\max}}\right)}-1}\left(e^{\beta\left(\frac{S(t)-S_c}{S_{\max}}\right)}-1\right) \tag{4}$$

where K_S is the hydraulic conductivity of the soil in saturated conditions and the dimensionless exponent is characteristic of the size and distribution of the pores in the soil. The evapotranspiration is assumed to be a function of the water content in the soil and potential evapotranspiration, calculated using the formulation of Hargreaves and Samani (1982).

Knowing the values of R, R_{sub}, and L, it is possible to model the surface, Q_{sur}, sub-surface, Q_{sub}, and deep flow, Q_g, routed contributions based on the conceptual framework of the linear reservoir at the closing section of a single sub-catchment. In the case of Q_{sur}, the value of the parameter k, which is a function of the residence time on the catchment slope, is estimated by relating the velocity to the average slope length. However, one of the challenges is to properly estimate the velocity, which should be calculated for each flood event (Rinaldo and Rodríguez-Iturbe, 1996). This velocity is a function of the effective rainfall intensity and the event duration (Rodríguez-Iturbe et al., 1982). In each sub-catchment, the runoff propagation is carried out based on the geomorphological theory of hydrologic response. The overall catchment travel time distributions are considered as nested convolutions of statistically independent travel time distributions along sequentially connected, objectively identified, smaller sub-catchments. Regarding Q_{sub} and Q_g, the value of k was calibrated, comparing the observed and simulated streamflow at Vicenza. Calibration of the hydrological model parameters was performed by AAWA, and is described in Ferri et al. (2012), which uses the time series of precipitation from 2000 to 2010 to minimize the root mean square error between observed and simulated values of water levels at the ARPAV (Veneto Region Environmental Protection Agency) gauged stations located along the river network (i.e., Bolzano Vicentino, Longare, Lugo di Vicenza, Montegalda, Ponte Marchese, S. Agostino and Vicenza).

Based on requirements in Article 6 of the 2007/60/CE Flood Directive (EU, 2007), the hydrological and hydraulic models described above were used to run three hazard scenarios as part of the Flood Risk Management Plan of the Eastern Alps Hydrographic District:

1. A flood with a low probability, which is 300-year return period in this area;
2. A flood with a medium probability, which is a 100-year return period in this area; and
3. A flood with a high probability, which is a 30-year return period in this area.

As a compromise between computational burden and result validity, the following modeling hypotheses were assumed for evaluating the hydrographs of the three return periods:

1. The return period refers to the rainfall volume at a certain time step. This simplification was applied to avoid having to consider the cumulative probability of multiple variables, such as temperature, snow water equivalent, soil moisture conditions and status of the levees during the weather event;
2. The hydrological model did not run in continuous mode but on an event basis;
3. Snow accumulation/melting and evapotranspiration processes were not simulated;
4. The initial conditions of the variables, which affected the estimation of effective rainfall, were determined by calibration, considering the heaviest rainfall event ever recorded in the catchment under investigation as the reference scenario. This approach allows for the potential underestimation due to the simplifications assumed in point 3 to be taken into account.

To estimate the Intensity-Duration-Frequency (IDF) curves associated with different return periods, a Gumbel distribution was applied to the rain gauge data covering a sufficiently long time period (i.e., at least 20 years) to guarantee the statistical significance of the outputs. The hyetograph shapes were determined by considering the trends of past extreme weather events that occurred in the territory. They were generated by assuming the following shapes: uniform; monotone increasing; triangular isosceles; and double peak; and were the result of a random binomial multiplicative process (Gupta and Waymire, 1993). Based on the results of simulations with different flood events, the reference hydrograph for an assigned return time was chosen based on maximum values at the peak while maintaining an adequate volume.

Table S1: The land use classes used in the calculations of flood exposure and vulnerability

ID	Description
1	Residential
2	Hospital facilities, health care, social assistance
3	Buildings for public services
4	Commercial and artisan
5	Industrial
6	Specialized agricultural
7	Woods, meadows, pastures, cemeteries, urban parks, hobby agriculture
8	Tourist-Recreation
9	Unproductive
10	Ski areas, Golf course, Horse riding
11	Campsites
12	Communication and transportation networks: roads of primary importance
13	Communication and transportation networks: roads of secondary importance
14	Railway area
15	Area for tourist facilities, Zone for collective equipment (supra-municipal, subsoil)
16	Technological and service networks
17	Facilities supporting communication/transportation networks (airports, ports, service areas, parking lots)
18	Area for energy production
19	Landfills, Waste treatment plants, Mining areas, Purifiers
20	Areas on which plants are installed as per Annex I of Legislative Decree 18 February 2005, n. 59
21	Areas of historical, cultural and archaeological importance; cultural heritage
22	Environmental goods
23	Military zone

The Citizen Observatory (CO) for Flood Risk Management has an estimated cost of around 5 million Euros. Table S2 provides a breakdown of these costs.

Table S2: The costs of the components of the Citizen Observatory (CO) for Flood Risk Management

Component of the CO	Cost (€)
Purchase and installation of sensors for environmental monitoring (including 5 year maintenance)	1 000 000
Implementation of a forecasting system coupled with a data assimilation module (including 5 year maintenance, hardware, software licences)	750 000
Implementation of a decision support IT platform for sensor data storage, alarm setting, communication services (including 5 year maintenance)	600 000
Implementation of information and communication campaigns aimed at the participants of the CO (citizens, students) for maintaining their involvement and improving their flood risk awareness and preparedness (5 year program)	860 000
Expert involvement of technicians in the environmental monitoring of floods (5 year duration)	400 000
Total cost including administrative costs, incentives and VAT (22%)	**4 900 000**

Table S3: Maximum flood damage values (€ / m^2) per damage category (Huizinga, 2007)

Region/country	Residential building	Commerce	Industry	Road	Agriculture
EU27	575	476	409	18	0.59
Italy	618	511	440	20	0.63
Luxembourg	1443	1195	1028	46	1.28
Germany	666	551	474	21	0.68
Netherlands	747	619	532	24	0.77
France	646	535	460	21	0.66
Bulgaria	191	158	136	6	0.20

Table S4: Model assumptions and sources of uncertainties

<table>
<tr><th colspan="2">Component</th><th>Assumptions/Sources of uncertainty</th><th>Source of data or assumptions</th><th>Explanations and implications</th></tr>
<tr><td>Flood hazard</td><td>Area and depth flooded, flow velocity</td><td>The model is applied to all areas that could be affected by river flooding and/or a failure of the levees during a flooding event of a certain probability. Concerning the possible failure of the levees, water infiltration (i.e., siphoning) is not considered; a failure was simulated in the situation where the difference between the water level in the river and the embankment level was less than 20 cm (as a precaution in relation to the unknown geotechnical characteristics and the possible uncertainty related to the elevation profile).

The values *h* of the maximum water depth and *v* of the maximum flow velocity that occur during an overflow event are well-known at each point; the hazard is correlated to the intensity of the phenomenon, which is a function of the depth and velocity. For the risk assessment, hazard is represented in relative terms in the interval between 0 and 1 so three classes are defined (the function described below is generally formulated by taking the safety of people, as a vulnerable element, into account): Low Hazard (H_l), medium Hazard (H_m), and high Hazard (H_h).

<table><tr><th>Description</th><th>Hazard classes</th><th>Hazard values</th></tr><tr><td>Flooded areas with low water depth:
$h \leq 1$ m if $v \leq 0.5$ m/s
$hv \leq 0.5$ m^2/s if $v > 0.5$ m/s</td><td>H_l</td><td>0.4</td></tr><tr><td>Flooded areas with significant water depth and/or relevant flow velocity:
$1 < h \leq 2$m if $v \leq 0.5$ m/s
$0.5 < hv \leq 1$ m^2/s if $v > 0.5$ m/s</td><td>H_m</td><td>0.8</td></tr><tr><td>Flooded areas with deep water and/or high flow velocity:
$h > 2$m if $v \leq 0.5$ m/s
$hv > 1$ m^2/s if $v > 0.5$ m/s</td><td>H_h</td><td>1.0</td></tr></table></td><td>Hydrological-hydraulic modelling (HEC-RAS)

Hazard classes are defined on the basis of a strictly qualitative evaluation, from an assessment made by the Provincia Autonoma di Trento (2006)</td><td>The levee breakpoints were identified by the hydraulic model based on the reference hydrograph (for the 3 different return times) and assessed, taking the height of the levees as well as the possible presence of banks or floodplains into account. The number of levee failure scenarios that were simulated along a critical section was based on the length of the river section and on historical evidence. The purpose of the investigation was not so much to analyze levee breaches from a geotechnical point of view, but to determine the effects in terms of the "propensity to flood" the area. In the situation of overlapping breaches, the maximum values for the variables *h* and *v* were assumed.

Hazard values do not change with the implementation of the citizen observatory and hence remain constant in the analysis.</td></tr>
</table>

Component		Assumptions/Sources of uncertainty	Source of data or assumptions	Explanations and implications
Flood exposure	People affected	Relative values of exposure range from 0.9 to 1, increasing as the population density increases	ISPRA (2012)	Rather than assuming exposure is 1 if any people are present, this assumption decreases the exposure as the population density decreases, thereby decreasing the overall risk. Moreover, these exposure values do not change with the implementation of a citizen observatory and hence remain constant in the analysis.
	Economic activities affected	Relative values of exposure by land use type were based on restoration costs resulting from losses in production and services	Costs provided by the Provincia Autonoma di Trento (2006) and values derived through expert consultation	These relative values are based on decades of experience with understanding exposure related to flood risk and hence are conservative estimates. These exposure values remain constant in the analysis.
	Environmental and cultural assets affected	Relative values of exposure by land use type were based on restoration costs resulting from potential damage		
Flood vulnerability	People affected – physical vulnerability	Relative vulnerability is based on instability of people in flowing water, derived from a flood hazard rating and debris factor from laboratory experiments.	DEFRA and UK Environment Agency (2006) ISPRA (2012)	Relative vulnerability is generally low (0.25) except under conditions when the combination of water height and flow velocity are appreciable. These values remain constant in the analysis.
	People affected – social vulnerability	The carrying capacity (weighted 0.4) and the adaptive capacity (weighted 0.6) are comprised of 10 individual weighted components. These components are expressed by value functions.	Value functions, values and weights derived through expert consultation	Values are conservative estimates based on expert consultation and local context. They will affect the final result, but they can only be validated/modified once the citizen observatory becomes operational.
	Economic activities affected	Functions for relative vulnerability of buildings, roads, vineyards, orchards and olive trees, vegetables, natural and semi-natural environments were derived based on laboratory experiments.	Clausen and Clark (1990) Lab experiments by Risk Frontiers Citeau (2003)	Relative vulnerability is generally low (0.25) except under conditions when the combination of water height and flow velocity are appreciable except for agricultural areas where relative vulnerability starts at the higher level of 0.5. These values remain constant in the analysis.
	Environmental and cultural assets affected	Vulnerability is 1 if protected areas are susceptible to nitrate pollution (land use 20) or there is presence of a pollution source (land use type 8 and 22). When no pollution source present, vulnerability is 0.25 if the flow velocity is ≤ 0.5 m/s and water height is ≤ to 1 m; otherwise 0.5.	AAWA with expert consultation	In the absence of specific studies, it was assumed that the indirect environmental vulnerability, i.e. that resulting from the consequent loss of functionality due to flooding, is equal to 0.25. Hence, relative vulnerability is generally low (0.25) except under conditions when the combination of water height and flow velocity are appreciable. It affects only a few land-use types, and these values remain constant in the analysis.
		Vulnerability is 1 if an area contains assets related to cultural heritage (land use 21).	ISPRA (2012)	It affects only land use type 21 and remains constant in the analysis.
Risk		The macro-category ‘people affected’ is weighted 10 times greater than the other two (i.e., economic activities affected and environment and cultural assets affected).	Stakeholder interviews undertaken by AAWA	This weighting reflects the importance of the safety of people in the risk calculation.

Component	Assumptions/Sources of uncertainty	Source of data or assumptions	Explanations and implications
Costs of flood damage	Damage estimates by damage category were estimated for each country in the EU including Italy (Table S3).	Huizinga (2007)	These figures come from a study by Huizinga (2007) from the Joint Research Center (JRC) in Italy. In 2017, Huizinga et al. (2017) published a report on global flood depth damage functions, comparing the results in 2017 with those in 2007. The overall patterns matched the 2017 values but showed overestimates in Europe, which were corrected by assuming a 40% inalterable portion for European buildings. The numbers then matched well. Hence some uncertainty analysis has been performed by the original authors of the figures. We would also assume they are conservative, having been published in 2007.

Figure S1: Value functions for the vulnerability indicators to evaluate the Coping Capacity (De Luca, 2013)

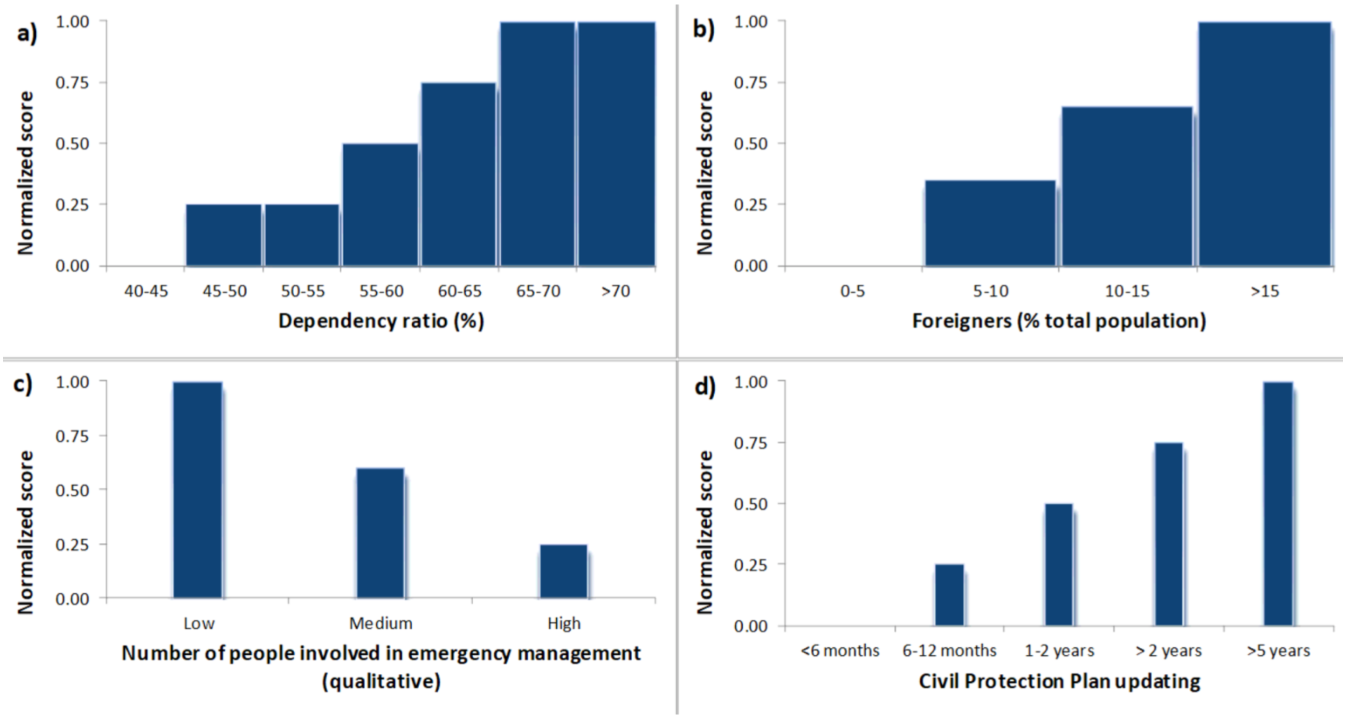

Figure S2: Value functions for the vulnerability indicators related to the Early Warning System (EWS) and Adaptive Capacity: a) reliability, b) lead time, and c) information content (De Luca, 2013)

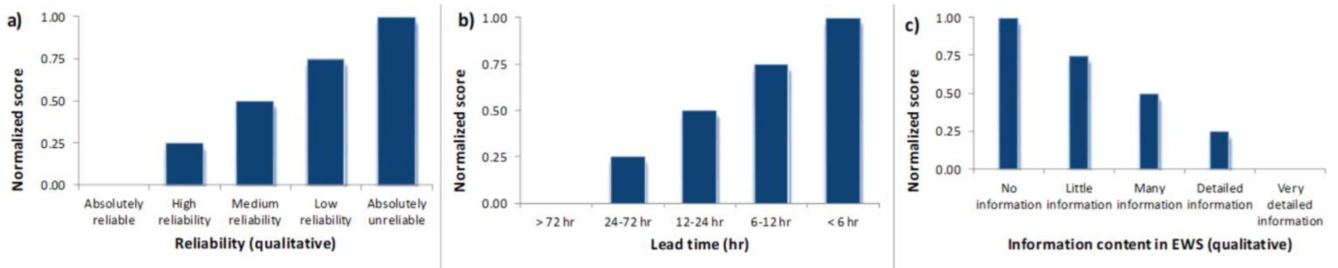

Figure S3: Value functions for the vulnerability indicators that are part of evaluating the Adaptive Capacity (De Luca, 2013)

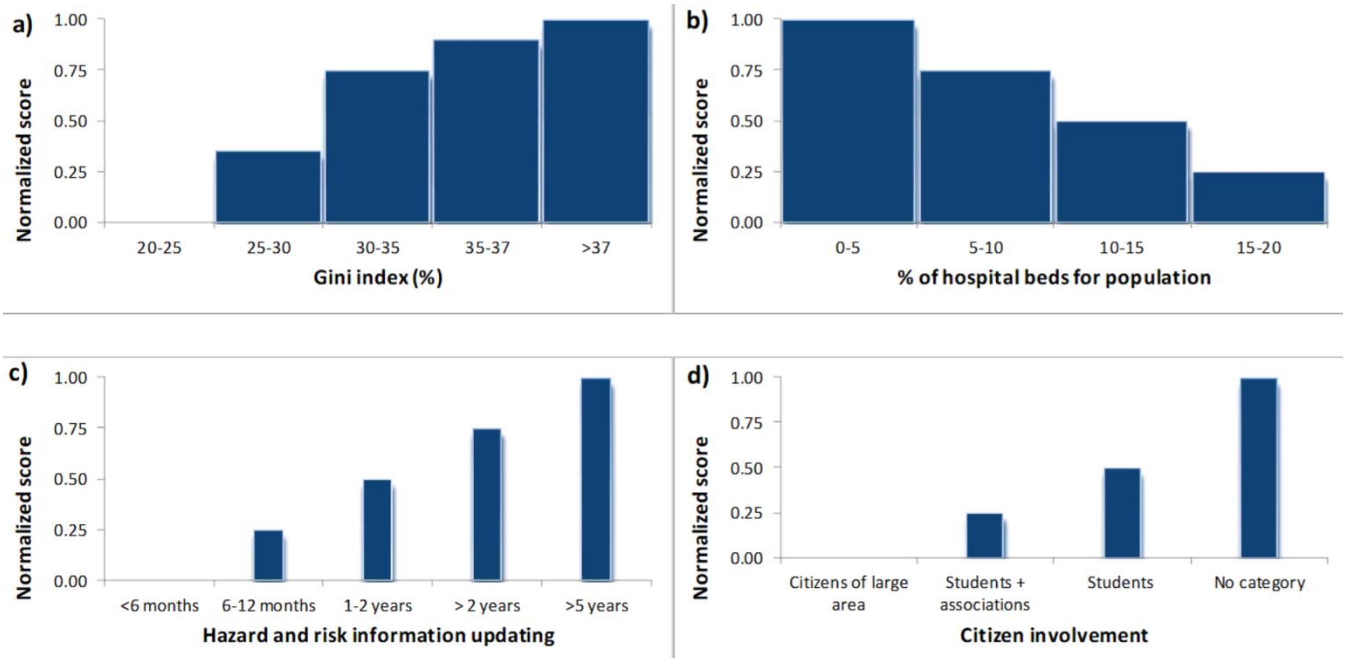

Figure S4: Vulnerability values of buildings as a function of water height (*h*) and flow velocity (*v*)

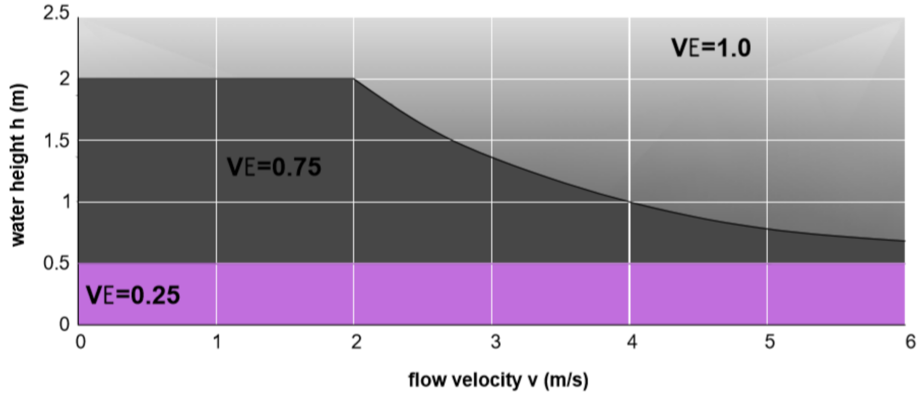

Figure S5: Vulnerability values of the network infrastructure as a function of water height (*h*) and flow velocity (*v*)

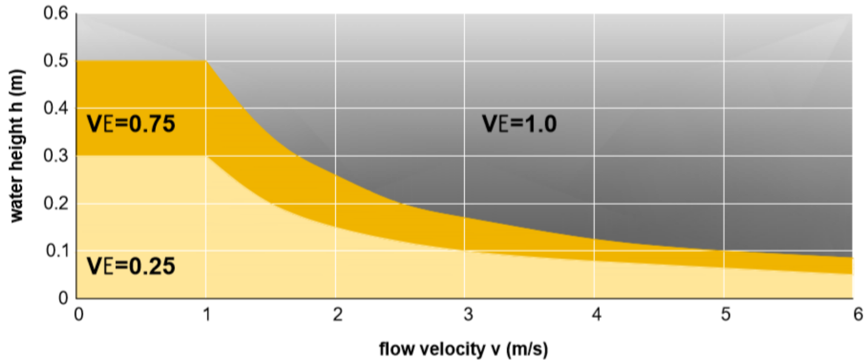

Figure S6: Vulnerability values as a function of the water height (*h*) and the flow velocity (*v*) for: (a) vineyards, (b) orchard and olive trees, (c) vegetables, and (d) natural and semi-natural environments, derived from laboratory experiments (Citeau, 2003)

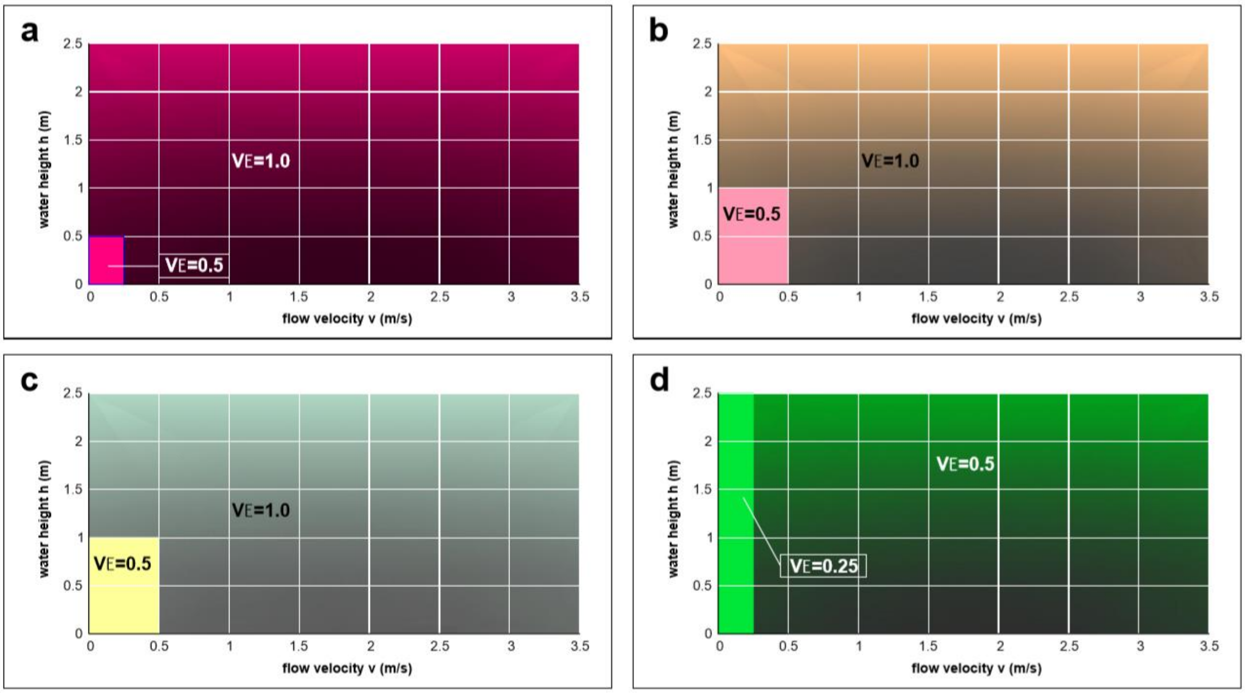

References

Citeau, J.-M.: A New Control Concept in the Oise Catchment Area. Definition and Assessment of Flood Compatible Agricultural Activities, FIG working week, Paris, France., 2003.

Clausen, L. and Clark, P. B.: The development of criteria for predicting dambreak flood damages using modelling of historical dam failures, in Proceedings of the International Conference on River Flood Hydraulics. 17-20 September 1990., edited by W. R. White, pp. 369–380, John Wiley & Sons Ltd. and Hydraulics Research Limited., 1990.

De Luca, C.: Integrated Environmental and Socio-economic Assessment of Flood Risk in GIS Context in the Vipacco Basin, Tesi Magistrale, Università di Ca Foscari, Anno Accademico 2012/2013, 2013.

DEFRA and UK Environment Agency: Flood and Coastal Defence R&D Program: Flood Risk to People, Phase 2, FD2321/TR2 Guidance Document., 2006.

EU: Directive 2007/60/EC of the European Parliament and of the Council of 23 October 2007 on the assessment and management of flood risks. Available at: https://eur-lex.europa.eu/legal-content/EN/TXT/?uri=CELEX:32007L0060, 2007.

Ferri, M., Monego, M., Norbiato, D., Baruffi, F., Toffolon, C. and Casarin, R.: La piattaforma previsionale per i bacini idrografici del Nord Est Adriatico (I), in Proceedings of XXXIII Conference on Hydraulics and Hydraulic Engineering, Brescia, Italy., 2012.

Gupta, V. K. and Waymire, E. C.: A statistical analysis of mesoscale rainfall as a random cascade, J. Appl. Meteor., 32(2), 251–267, doi:10.1175/1520-0450(1993)032<0251:ASAOMR>2.0.CO;2, 1993.

Hargreaves, G. H. and Samani, Z. A.: Estimating potential evapotranspiration, Journal of the Irrigation and Drainage Division, 108(3), 225–230, 1982.

Huizinga, H. J.: Flood damage functions for EU member states. Technical Report, HKV Consultants. Implemented in the framework of the contract #382441-F1SC awarded by the European Commission - Joint Research Centre, 2007.

Huizinga, H. J., Moel, H. de and Szewczyk, W.: Global flood depth-damage functions. Methodology and the database with guidelines. EUR 28552 EN. doi: 10.2760/16510, 2017.

ISPRA: Proposta metodologica per l'aggiornamento delle mappe di pericolosità e di rischio. Attuazione della Direttiva 2007/60/CE/ relative alla valutazione e alla gestione dei rischi da alluvioni (Decreto Legislativo n.49/2010). Istituto Superiore per la Protezione e la Ricerca Ambientale (ISPRA), Roma., 2012.

Laio, F., Porporato, A., Ridolfi, L. and Rodriguez-Iturbe, I.: Plants in water-controlled ecosystems: active role in hydrologic processes and response to water stress, Advances in Water Resources, 24(7), 707–723, doi:10.1016/S0309-1708(01)00005-7, 2001.

Mazzoleni, M., Verlaan, M., Alfonso, L., Monego, M., Norbiato, D., Ferri, M. and Solomatine, D. P.: Can assimilation of crowdsourced data in hydrological modelling improve flood prediction?, Hydrol. Earth Syst. Sci., 21(2), 839–861, doi:10.5194/hess-21-839-2017, 2017.

Mazzoleni, M., Cortes Arevalo, V. J., Wehn, U., Alfonso, L., Norbiato, D., Monego, M., Ferri, M. and Solomatine, D. P.: Exploring the influence of citizen involvement on the assimilation of crowdsourced observations: a modelling study based on the 2013 flood event in the Bacchiglione catchment (Italy), Hydrol. Earth Syst. Sci., 22(1), 391–416, doi:10.5194/hess-22-391-2018, 2018.

Provincia Autonoma di Trento: Piano Generale di Utilizzazione delle Acque Pubbliche, Parte IV, DPR 15/02/2006., 2006.

Rinaldo, A. and Rodríguez-Iturbe, I.: Geomorphological theory of the hydrological response, Hydrological Processes, 10(6), 803–829, doi:10.1002/(SICI)1099-1085(199606)10:6<803::AID-HYP373>3.0.CO;2-N, 1996.

Rodríguez-Iturbe, I., González-Sanabria, M. and Bras, R. L.: A geomorphoclimatic theory of the instantaneous unit hydrograph, Water Resour. Res., 18(4), 877–886, doi:10.1029/WR018i004p00877, 1982.

Tarboton, D. G. and Luce, C. H.: Utah energy balance snow accumulation and melt model (UEB), computer model technical description and users guide, Utah Water Research Laboratory, Utah State University and USDA Forest Service, Intermountain Research Station., 1996.